Am J Clin Exp Urol 2018;6(6):219-233
www.ajceu.us /ISSN:2330-1910/AJCEU0087541

Original Article

Concordant miRNA and mRNA expression profiles in humans and mice with bladder outlet obstruction

Ali Hashemi Gheinani[1,2*], Ivonne Köck[3*], Evalynn Vasquez[1,2,7*], Ulrich Baumgartner[4], Alexander Bigger-Allen[1,5], Bryan S Sack[1,2,8], Fiona C Burkhard[6], Rosalyn M Adam[1,2], Katia Monastyrskaya[3,6]

[1]Department of Urology, Boston Children's Hospital, Boston, MA, USA; [2]Department of Surgery, Harvard Medical School, Boston, MA, USA; [3]Urology Research Laboratory, Department of Clinical Research, University of Bern, Switzerland; [4]Institute of Pathology, University of Bern, Switzerland; [5]Biological and Biomedical Sciences PhD Program, Harvard Medical School, Boston, MA, USA; [6]Department of Urology, University Hospital, Bern, Switzerland; [7]Division of Urology, Children's Hospital Los Angeles and Keck School of Medicine of the University of Southern California, Los Angeles, CA 90027, USA; [8]Department of Urology, Mott Children's Hospital and University of Michigan, Ann Arbor, MI 48109, USA. [*]Equal contributors.

Received October 29, 2018; Accepted December 14, 2018; Epub December 20, 2018; Published December 30, 2018

Abstract: Bladder outlet obstruction (BOO) leads to lower urinary tract symptoms (LUTS) and urodynamic changes of the bladder function. Previously we identified microRNA (miRNA) and mRNA expression profiles associated with different states of BOO-induced LUTD in human patients. Bladder wall remodeling resulting from obstruction is widely studied in animal models of experimentally-induced partial BOO (pBOO). Here we determined the expression profiles of miRNAs and selected mRNAs in pBOO mice and compared the observed changes to human patients. Similar to results from human patients, we observed a down-regulation of smooth muscle-associated miRNAs mmu-miR-1, mmu-miR-143, mmu-miR-145, mmu-miR-486 and mmu-miR-133a in pBOO mouse bladders. Pro-fibrotic miRNAs mmu-miR-142-3p and mmu-miR-21 were up-regulated, and anti-fibrotic miRNA mmu-miR-29c was down-regulated. Pathway analysis in human BOO patients identified TNF-alpha as the top upstream regulator. Although there was evidence of hypertrophic changes in pBOO mice, contrary to human data, we observed no regulation of TNF-responsive genes in the mouse model. Experimentally-induced pBOO in mice led to significant gene expression changes, including alteration of pro-fibrotic mRNAs and miRNAs resembling human BOO patients. Gene expression changes were also validated in a mouse model of bladder inflammation. Lack of evidence of TNF-alpha-induced miRNA and mRNA regulation might indicate a different pathophysiological mechanism of organ remodeling in pBOO model compared to the human disease.

Keywords: Lower urinary tract symptoms, partial bladder outlet obstruction, fibrosis, pathway analysis

Introduction

Benign enlargement of the prostate in adult men leads to bladder outlet obstruction (BOO) and clinical lower urinary tract symptoms (LUTS), including urgency, frequency, nocturia and urinary retention. Animal models of BOO are widely used to gain insight into the molecular processes of organ remodeling since they enable precise control over the initiation of obstruction. In order to study bladder changes occurring during BOO, partial outlet obstruction (pBOO) is performed in laboratory animals, including mice, rats, rabbits, guinea pigs, dogs, and pigs (reviewed in [1]). The most common method to induce pBOO in rodents is by partial ligation of the proximal urethra [2, 3], that leads to increased intravesical pressure, compensatory hypertrophy and hyperplasia leading to an elevated bladder-to-body weight ratio and functional alterations consistent with those observed in human patients. With sustained obstruction, ongoing tissue remodeling characterized by dysregulated collagen deposition and fibrosis, as well as alterations in contractile proteins such as smooth muscle myosin heavy chain (SM-MHC) isoform leads to bladder decompensation, in which bladder contractility diminishes, resulting in loss of function (reviewed in [4]). Obstruction also causes changes in the bladder vasculature, including transient ischemia and hypoxia, and an increase in oxidative stress

[5-7]. The morphological, molecular and functional changes observed in animal models of pBOO mirror those seen in bladder tissues from patients with obstruction-related lower urinary tract obstruction, demonstrating the validity of such models for mechanistic interrogation of the molecular basis of the response to obstruction.

Although the gross morphological and functional consequences of pBOO in animal models and BOO in humans are well characterized, the epigenetic drivers of such changes are incompletely defined. MicroRNAs have essential biological functions in development and homeostasis. Dysregulation of miRNAs contributes to many human diseases [8], including LUTD [9]. MiRNAs have been implicated in bladder pathologies including bladder pain syndrome [10, 11], inflammation-induced overactivity [12] and the response to outlet obstruction in rodents and humans [13-16]. MiRNAs have also been shown to regulate specific cellular phenotypes within the urinary tract, including smooth muscle cell proliferation [17] and regulation of urothelial permeability [11]. The miR-29 family of miRNAs, known to target extracellular matrix proteins [18], was found to be downregulated following outlet obstruction in rodents and humans [13]. The reduction of miR-29 led to derepression and upregulation of multiple ECM-associated mRNAs, as well as a corresponding increase in bladder stiffness. Obstruction also increased expression of the transcriptional regulators c-Myc, NFκB and Smad3 which in turn are known to repress miR-29b and miR-29c [19, 20], demonstrating the existence of complex feedback relationships between miRNAs and the mRNAs they target. Integrated analysis of differentially expressed miRNAs and mRNAs from human patients with discrete urodynamically defined phenotypes of BOO identified tumor necrosis factor-alpha (TNF-α) as the top upstream signaling pathway regulator [14]. It has been shown that in bladder smooth muscle cells treated with TNF-α, miRNA miR-199a-5p was significantly attenuated, leading to a compensatory increase in NFκB signaling activity [21]. miR-30, a known regulator of the profibrotic molecule CTGF, was also found to be downregulated following obstruction [22]. CTGF has been implicated as a driver of fibrosis in a variety of organs including the bladder subjected to either anatomic or functional obstruction [23, 24]. The miR-145 family has also been implicated in the regulation of smooth muscle phenotype (reviewed in [25]). MiRNA-145 is one of the most highly expressed miRNAs in hollow organ smooth muscle, and its downregulation secondary to genetic deletion of the miRNA processing enzyme Dicer was associated with altered bladder contractility due in part to reduced expression of L-type calcium channels [26], and with diminished remodeling of vascular smooth muscle in response to injury as a result of deficits in the actin cytoskeleton and decreased SMC migration [27]. Together, these studies demonstrate that in response to injury many miRNAs in animals and humans are perturbed, leading to transcriptional changes that promote hypertrophy, hyperplasia, fibrosis and functional deficits.

Recently, we performed quantitative transcriptome and miRNA profiling of different functional phenotypes of BOO-induced LUTDs in human patients [14]. Animal models of experimentally-induced pBOO allow longitudinal studies and might be better suited for further investigations of BOO development and detrusor instability [28]. In this study, we interrogated transcriptional and miRNA changes in the context of disease progression. Mice were subjected to pBOO for up to 8 weeks, the expression profiles of miRNAs and selected mRNAs were determined, and observed changes were compared to those in human patients with obstruction.

Materials and methods

Study approval

All animal studies were performed with approval from the Boston Children's Hospital Animal Care and Use Committee and with strict adherence to US Public Health Service and Office of Laboratory Animal Welfare guidelines. Approval to perform human urodynamics analyses and bladder biopsies was granted from the local Ethics Committee, University Hospital Bern, Bern, Switzerland (KEK 146/05), and all subjects provided written informed consent.

Creation of partial bladder outlet obstruction (pBOO)

All experiments were performed using 10-to-12-week-old male mice that were anesthetized with isoflurane and underwent microsurgical creation of pBOO essentially as described recently by us [29]. Briefly, anesthetized mice

Table 1. Bladder and body weights of sham versus obstructed mice

A. Bladder and body weights of mice subjected to pBOO or sham operation						
Condition	2 wk Body (g)	2 wk Bladder (g)	4 wk Body (g)	4 wk Bladder (g)	6 wk Body (g)	6 wk Bladder (g)
Sham	24.70	0.0189	26.90	0.0272	27.30	0.0237
	26.30	0.0232	29.70	0.0262	30.10	0.0264
pBOO	27.60	0.0536	29.90	0.0399	27.50	0.0299
	27.41	0.0268	29.00	0.0318	29.40	0.0366
	26.80	0.0586	28.10	0.0346	28.80	0.0527
B. Bladder-to-body weight ratio of mice subjected to pBOO or sham operation						
Condition	2 wk Ratio	2 wk Average	4 wk Ratio	4 wk Average	6 wk Ratio	6 wk Average
Sham	7.65E-04	8.24E-04	1.01E-03	9.47E-04	8.68E-04	8.73E-04
	8.82E-04		8.82E-04		8.77E-04	
pBOO	1.94E-03	1.70E-03	1.33E-03	1.22E-03	1.09E-03	1.39E-03
	9.78E-04		1.10E-03		1.24E-03	
	2.19E-03		1.23E-03		1.83E-03	

underwent a 1 cm laparotomy to expose the bladder and prostate. The prostatic lobes were bisected in the midline to expose the proximal urethra and bladder neck. A right-angle instrument was used to isolate the urethra and pass a 5-0 silk suture behind the urethra approximately 1 mm inferior to the bladder neck. Polyethylene tubing (PE10) with an outer diameter of 0.024 inches, was placed was placed periurethrally to prevent complete occlusion of the urethra. The 5-0 silk suture was then tied down over the tubing. Once the tubing was removed, the bladder was manually expressed to ensure a complete obstruction was not inadvertently created. The muscle layer was closed with 4-0 monocryl suture, and skin was closed using 9 mm stainless steel clips. Meloxicam was administered for 72 h. The sham procedure was identical except the 5-0 silk suture was not secured around the urethra. Sham surgery and pBOO was done in wildtype (WT) C57BL/6 mice and the bladders were harvested for the 1st study after 2, 4, 6 weeks and for the 2nd study after 2, 4, 6, and 8 weeks after surgery.

Cyclophosphamide model of bladder inflammation

To induce inflammation in the bladder, C57BL/6 mice at 9 wk of age were administered cyclophosphamide (Cyp) at 100 (low dose) or 300 (high dose) μg/g body weight by intraperitoneal injection. Mice receiving saline vehicle were included as controls. At 24 or 96 h following Cyp or vehicle injection, bladders were harvested, mucosa and detrusor tissues separated by microdissection and tissues processed for RNA or protein isolation, as described below.

Tissue harvest, RNA and protein isolation

Mice were euthanized at the indicated times following surgery. At the time of sacrifice, total body weight and bladder mass were recorded. All tissues used for molecular analysis were stored in RNAlater or immediately snap-frozen in liquid nitrogen. Total RNA and protein was extracted with the mirVana Paris isolation kit (Applied Biosystems) from whole frozen mice bladders, which were stored in RNA*later* (Ambion). For sample disruption, RNA*later* was removed, cell disruption buffer was added, and the tissue was crushed with a motorized rotor-stator homogenizer. From the homogenized lysate total RNA and protein was isolated as described in the manufacturer's manual. Tissues from cyclophosphamide- or vehicle-treated mice were snap frozen in liquid nitrogen. Protein lysates were generated using FastPrep matrices (MP Biomedical) in lysis buffer (Cell Signaling Technology) whereas RNA was isolated following homogenization of tissues using FastPrep matrices in TRIzol (ThermoFisher), and purification of RNA using RNeasy columns (Qiagen). mRNA concentrations were measured by NanoDrop 2000 (ThermoFisher) and protein by BCA protein assay (Pierce).

Quantitative RT-PCR

The reverse-transcription reactions were carried out using High-Capacity cDNA Reverse

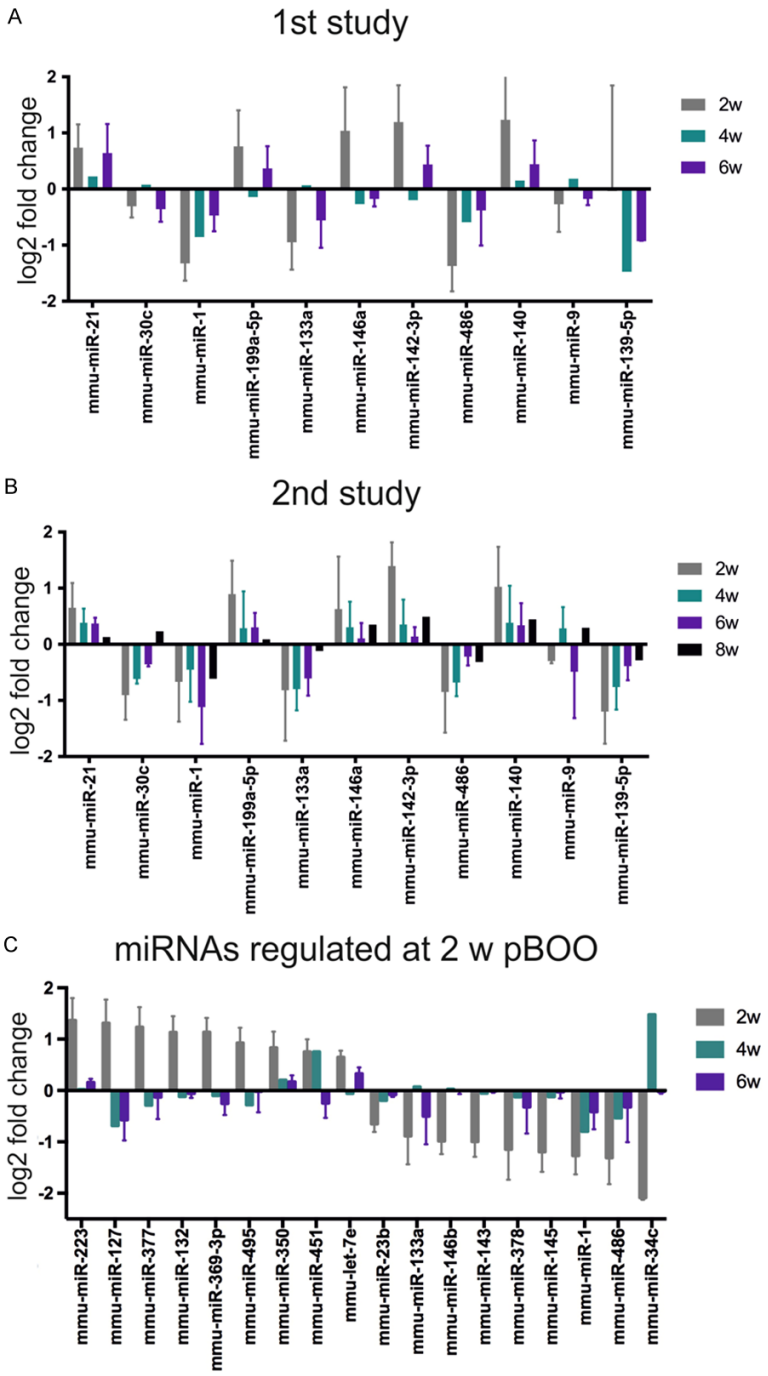

Figure 1. miRNA profiling in mouse bladders with pBOO relative to shams. NanoString nCounter miRNA assays were used to evaluate the expression of 598 mouse miRNAs (full data in Supplementary File). Bladder samples from the 1st and 2nd pBOO study were used and miRNA expression compared. Expression profiles of 11 MiRNAs, which were significantly regulated in human BOO patients' biopsies, is shown for the 1st study (A) and the 2nd study (B). MiRNA expression changes between 2 weeks obstruction and sham-operated mice were not significant. (C) MiRNA expression of the 1st study from miRNAs that are significantly ($P<0.05$) regulated at 2 weeks of obstruction compared to sham. Only miRNAs with a read number >100, log2>0.51 were used. Sham-operated mice (n=2/time point), 2 weeks, 4 weeks, 6 weeks (n=3/group), 8 weeks (n=7). Data are represented as mean ± SD. Expression changes at the later time points were not significant.

Transcription Kit (mRNA). TaqMan mouse gene expression assays were used to study the mRNA expression. Quantitative real-time PCR (qRT-PCR) was carried out in triplicates using the QuantStudio 3 Fast Real-time PCR System (Applied Biosystems). Ct values obtained after qRT-PCR were normalized to 18 s rRNA. Fold differences compared to the controls (sham-operated, same time point) were calculated.

miRNA expression profiling with NanoString

Expression profiles of 598 mouse miRNAs were established using NanoString mouse miRNA assays. 300 ng total RNA was analyzed using the nCounter Mouse v1.5 miRNA Expression Assay Kit (GXA-MMIR15-12) (NanoString, Seattle, WA, USA) according to manufacturer's instruction. Positive and negative control subtraction and normalization of raw data were performed using "NanoStringNorm" and "NanoStringDiff" R packages (available in CRAN) and expression profiling was performed using "EdgeR" from the R statistical environment (v.3.3.2) as previously described [30].

Statistical and data analysis

Results were presented as the mean ± standard deviation (SD). The level of significance was established at $\alpha=0.05$. To determine statistical significance One- and two-way ANOVA were used by GraphPad Prism 7 software (GraphPad). For data displaying a non-Gaussian distribution, the Kruskal-Wallis test was employed, with significance set at 0.05.

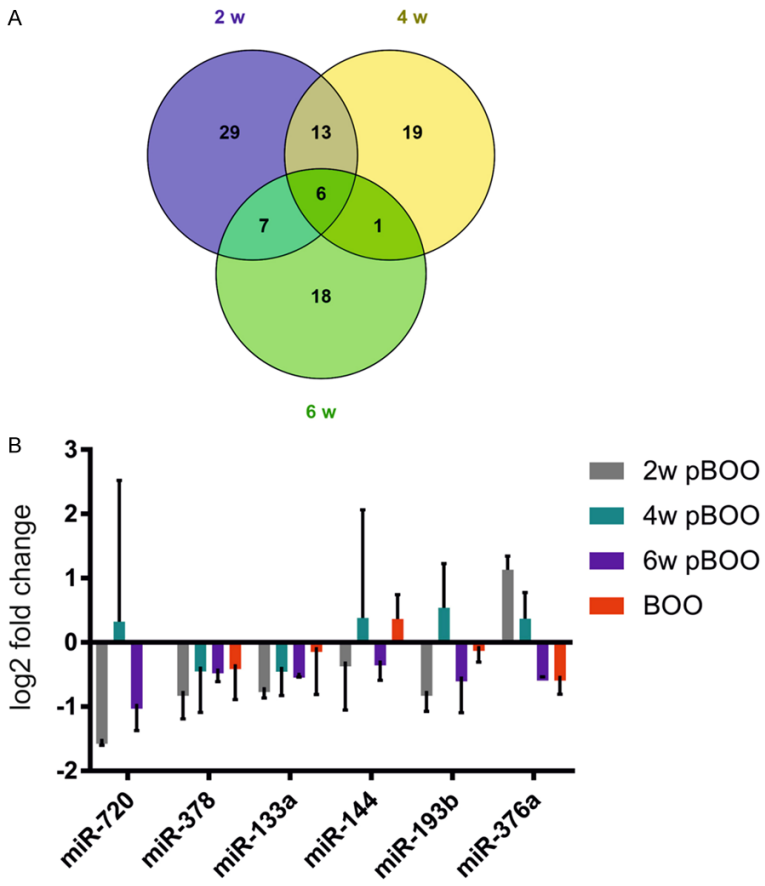

Figure 2. Common miRNAs, changed at 2, 4 and 6 weeks of pBOO, compared to BOO patients. A. Venn diagram of regulated miRNAs (read number >100, ABS log2>0.51) at 2, 4 and 6 weeks pBOO. B. Six miRNAs, regulated at all time points in pBOO mice compared with patient's data. Sham-operated mice (n=2/time point), 2 weeks, 4 weeks, 6 weeks (n=3/group), 8 weeks (n=7), BOO (n=18). Data are represented as mean ± SD.

Results

Structural changes in the bladder following pBOO

The bladders of mice with surgically-induced pBOO showed an increase in bladder size compared to sham-operated mice, that was evident in the increased bladder-to-body weight ratio (**Table 1**). The increase of the bladder-to-body weight ratio is consistent with studies from our group and others of bladder obstruction that demonstrate hypertrophy/hyperplasia within the bladder wall along with increased deposition of extracellular matrix (ECM) [3, 23, 29, 31].

Strong dysregulation of miRNAs 2 weeks after pBOO

To investigate whether the miRNA expression in obstructed mouse bladders is comparable with the previously reported patients' study [14], a NanoString nCounter miRNA assay was performed (Supplementary File). Among the miRNAs, which were altered after 2 weeks of pBOO compared to sham-operated animals in both studies we chose miRNAs known to play a role in bladder hypertrophy. At 2 week pBOO all miRNAs were similarly expressed in both studies, although the data for the 2nd study were more stable. Despite the increase in muscle contractility known to occur at 2 weeks following pBOO [29], the muscle-specific miRNA mmu-miR-1 and mmu-miR-133a were down-regulated in both studies between 2 and 8 weeks of obstruction. In both studies, as obstruction progressed, many of the initially regulated miRNAs gradually returned to the sham levels, including miR-146a, miR-9 (**Figure 1A**), from 1st study and mmu-miR-396, let-7e, miR-378, miR-21, and miR-199a-5p (**Figure 1B**) from the 2nd study. To further confirm these results, in the first study we selected 9 miRNAs, significantly up- or down-regulated at 2 weeks pBOO and followed their expression levels at the later time points (4 and 6 weeks of pBOO). In the majority of cases, the expression levels returned to control values, or became regulated in the opposite direction as obstruction progressed (**Figure 1C**). MiR-133a, -1, -486 and -let-7e retained their regulation, however, in all cases there was a significant reduction of the fold change values, indicating the trend towards weakening of alterations (**Figure 1C**).

Common miRNAs regulated at 2, 4 and 6 weeks of pBOO and in BOO patients

Of all miRNAs, regulated in the 2nd study, six were shared between 2-, 4- and 6-week time points (**Figure 2A**), so we investigated whether they were regulated in all BOO patients, irrespective of their contractile phenotype. We determined the levels of these miRNAs in BOO

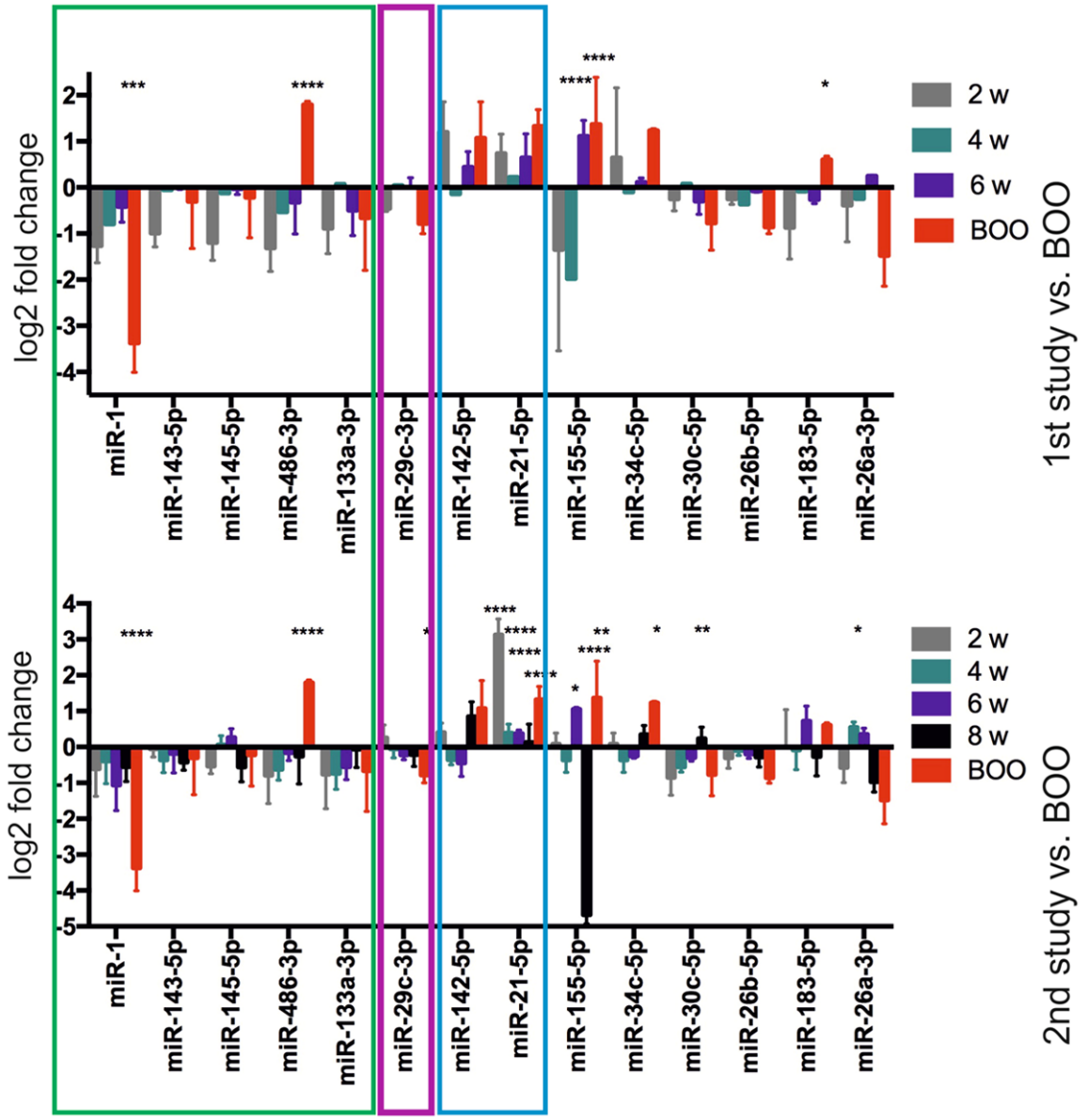

Figure 3. Regulation of miRNAs, relevant for bladder remodeling during pBOO and BOO. Regulation of selected miRNAs in pBOO mouse bladders (1st and 2nd study) was compared to the patients with BOO-induced LUTDs BOO. MiRNAs were chosen based on their role in bladder remodeling and hypertrophy. Sham-operated mice (n=2/time point), 2 weeks, 4 weeks, 6 weeks (n=3/group), 8 weeks (n=7), human BOO (n=18). Data are represented as mean ± SD, and expressed compared to 2 week pBOO time point. *P≤0.05, **P≤0.01, ****P≤0.0001. P>0.5 is not significant.

patients using the NGS miRNA data (n=18 patients vs n=6 controls) [14]. MiR-378 and miR-133a were down-regulated in all time-points of pBOO and in humans. MiR-193b, and miR-376a were up-regulated at 2 and 4 weeks pBOO and down-regulated at 6 weeks pBOO and in humans, while miR-144 was up-regulated at 4 week pBOO and in humans, and down-regulated at 2 and 6 weeks pBOO. Mmu-miR-720 was not expressed in humans (**Figure 2B**).

Regulation of important human miRNA orthologues in pBOO animal models

We investigated the levels mouse orthologues of several miRNA, significantly altered in human patients, in pBOO animals in both studies (**Figure 3**). Similar to results from human patients, we observed a down-regulation of smooth muscle-associated miRNAs miR-1, and miR-133a in pBOO mouse bladders (**Figure 3**, green

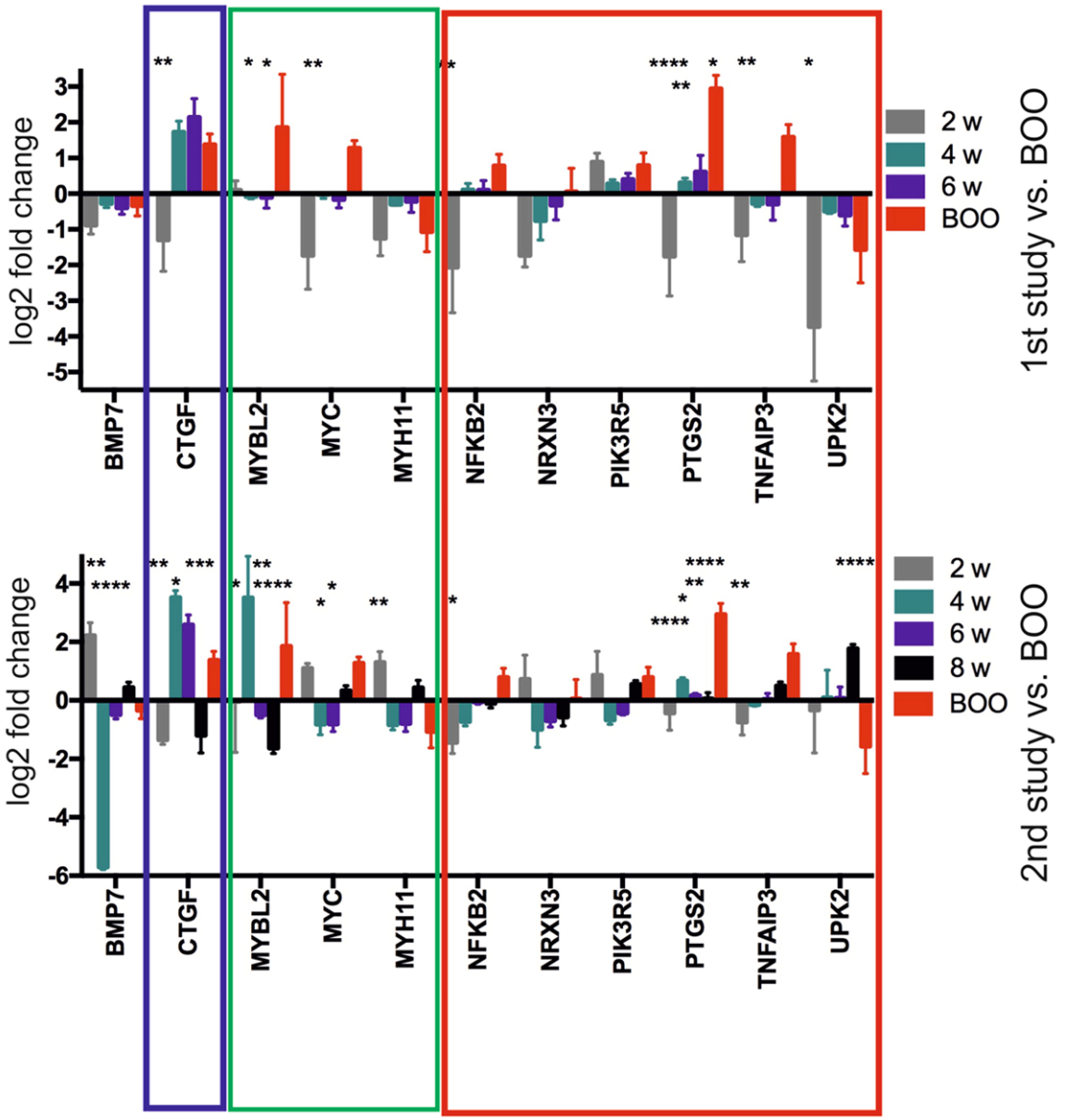

Figure 4. Gene expression of important pathway signaling elements in pBOO mice and humans with BOO. qRT-PCR was carried out to study the mRNA expression of 11 genes in 1st and 2nd study compared to human BOO data. Sham-operated mice (n=2/time-point), 2 weeks, 4 weeks, 6 weeks (n=3/group), 8 weeks (n=7), BOO (n=18). Data are represented as mean ± SD, and expressed relative to human BOO, read number >100, *P≤0.05, **P≤0.01, ***P≤0.001, ****P≤0.0001. P>0.5 is not significant.

frame). The muscle-associated miRNAs miR-143 and miR-145 were down-regulated just in 2 weeks of obstruction and miR-486 was reduced in mice but enhanced in patients. The anti-fibrotic miRNA miR-29c was down-regulated at 2 weeks of pBOO, and significantly so in BOO patients (**Figure 3**, purple frame). The pro-fibrotic miRNAs miR-142-3p and miR-21 (**Figure 3**, red frame) were up-regulated at 2 weeks in both studies, and variably at later time points (weeks 6 and/or 8). Interestingly, pro-inflammatory NFκB-induced miR-155, stably enhanced in humans, showed an inconsistent and sometimes bi-phasic expression pattern in pBOO mice. MiR-30c and -26b and the other tested miRNAs showed similar expression patterns between mice and humans (**Figure 3**).

Expression changes of important pathway elements in pBOO mice and human patients

Pathway analysis of the transcriptome data from human patients with BOO-induced LUTDs

Table 2. Bladder and body weights of mice subjected to cyclophosphamide or vehicle treatment

A. Bladder and body weights of mice subjected to Cyp or Veh treatment				
Condition	24 h Body (g)	24 h Bladder (g)	96 h Body (g)	96 h Bladder (g)
Veh	28.7	0.027	29.2	0.022
	28.6	0.028	27.3	0.022
	28.3	0.025	26.7	0.023
	27.7	0.020	29.7	0.023
Cyp-low	26.1	0.0191	27.0	0.020
	26.8	0.0192	27.9	0.021
	26.5	0.0195	28.5	0.021
	26.8	0.0168	25.6	0.017
Cyp-high	27.5	0.023	27.5	0.042
	24.2	0.047	24.2	0.039
	26.2	0.030	26.2	0.045
	26.4	0.035	26.4	0.030
B. Bladder-to-body weight ratio of mice subjected to Cyp or Veh treatment				
Condition	24 h Ratio	24 h Average	96 h Ratio	96 h Average
Veh	0.941	0.881±0.113	0.753	0.799±0.047
	0.979		0.806	
	0.883		0.861	
	0.722		0.774	
Cyp-low	0.732	0.703±0.051	0.741	0.724±0.040
	0.726		0.753	
	0.736		0.737	
	0.627		0.664	
Cyp-high	0.950	1.327±0.316*	1.527	1.498±0.253**
	1.722		1.612	
	1.299		1.718	
	1.336		1.136	

Veh, vehicle; Cyp-low (cyclophosphamide, 100 μg/g body weight); Cyp-high (cyclophosphamide, 300 μg/g body weight). *, P=0.034 vs 24 h Veh; **, P=0.0043 vs 96 h Veh, t-test.

identified TNF-α as the top upstream regulator and revealed signaling molecules, including MYC, FOS, CTGF, and PIK3R5, which were strongly induced in different urodynamic states of BOO [14]. Expression of 11 mRNAs, which were significantly regulated in human patient samples were investigated in mice with pBOO in both studies using qRT-PCR. We observed similarity in the expression profiles of CTGF, which was significantly up-regulated at 4 and 6 weeks pBOO in both studies and in humans (**Figure 4**, purple frame). In contrast, the significant up-regulation of MYC and MYB Proto-Oncogene Like 2 (MYBL2), observed in humans BOO patients, was not consistently reproduced in pBOO mice. Likewise, the smooth muscle-specific mRNAs myosin-heavy chain-11 (MYH11) was up-regulated at 2 weeks pBOO in the 2nd study; but down-regulated at the other time points and in humans (**Figure 4**, green frame). Importantly, contrary to human data, we observed no regulation of TNF-α responsive genes NFκB2, PIK3R5, PTGS2 and TNFAIP3 in the mouse model (**Figure 4**, red frame).

Selective upregulation of MYC in a mouse model of bladder inflammation

As noted above, pro-inflammatory miRNAs and mRNAs were selectively regulated following obstruction in humans and mice. As an independent test of the impact of inflammation on mRNAs identified as responsive to obstruction, we subjected mice to injection with cyclophosphamide (Cyp) to evoke an acute inflammatory response within the bladder [32]. The mean body weight was decreased after 96 h in both Cyp-low and Cyp-high treated mice, which was concomitant with a significant increase in their bladder-to-body ratio (**Table 2**). We observed time- and dose-dependent changes in expression of MYC, TNFAIP3, BMP7, NRXN3, VEGFA, PI3KR5, MYBL2, HIF1A, and NFκB mRNAs in response to Cyp, with differential responses observed between detrusor and mucosa. In the mucosa, the levels of NRXN3, PI3KR5, MYBL2 mRNA were downregulated at 24 h in mice treated with high-dose Cyp (300 mg/g body weight, P<0.05), whereas BMP7 mRNA was upregulated in mucosa at 24 h in response to low-dose Cyp (100 mg/g body weight, *P<0.05) (**Figure 5A**). In the detrusor, TNFAIP3, HIF1A, and NFκB mRNAs were downregulated at 96 h following Cyp treatment, irrespective of dose, whereas VEGFA was upregulated in response to high dose Cyp (**Figure 5B**). MYC mRNA and protein were also noted to increase at 96 h following Cyp treatment (**Figure 5C**).

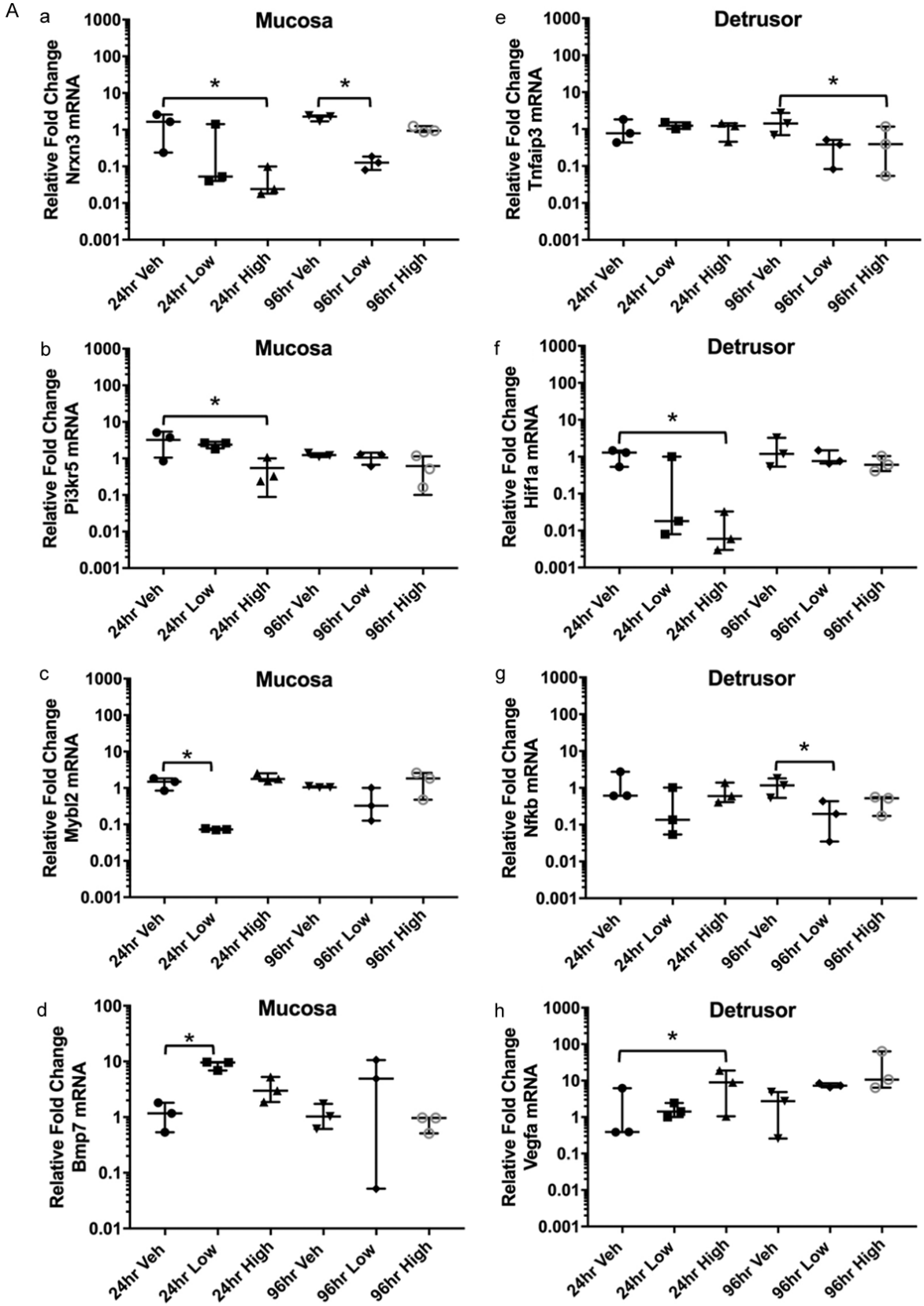
A
a
Mucosa
Relative Fold Change Nrxn3 mRNA
e
Detrusor
Relative Fold Change Tnfaip3 mRNA
b
Mucosa
Relative Fold Change Pi3kr5 mRNA
f
Detrusor
Relative Fold Change Hif1a mRNA
c
Mucosa
Relative Fold Change Mybl2 mRNA
g
Detrusor
Relative Fold Change Nfkb mRNA
d
Mucosa
Relative Fold Change Bmp7 mRNA
h
Detrusor
Relative Fold Change Vegfa mRNA
24hr Veh
24hr Low
24hr High
96hr Veh
96hr Low
96hr High

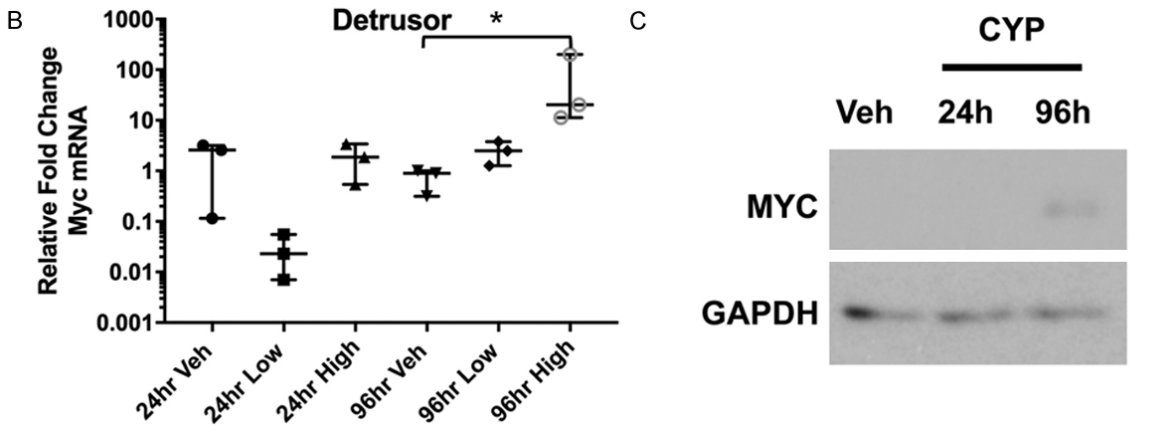

Figure 5. Cyclophosphamide (CYP)-induced hemorrhagic cystitis in mice induces upregulation of MYC. A. Differential sensitivity of obstruction-sensitive gene expression to Cyp. Data are presented as fold change relative to vehicle at each time point (*, P<0.05, Kruskal-Wallis test). B. Upregulation of c-myc mRNA in the detrusor after 96 hr of high dose CYP compared to vehicle control (n=3/group, P<0.05, Kruskal-Wallis test). C. Upregulation of Myc mRNA and protein in the detrusor at 96 hr post high dose CYP treatment.

Hypoxia is induced early in pBOO and gradually subsides later following obstruction

Hypoxia-inducible factor (HIF) 1 is the major regulator of oxygen homeostatic processes within the cells. Mice with surgically-induced pBOO after 1 week showed an increase in hypoxia-responsive genes [33], therefore, in order to understand the driver of the miRNA dysregulation early in obstruction, we assessed the mRNA levels of hypoxia markers HIF1A, VEGFA and LDHA at different time points of pBOO. Our results show that in both studies the subunit HIF-1α is significantly up-regulated after the first 2 weeks of obstruction but after 6 to 8 weeks its levels decrease, though HIF-1A is significantly up-regulated in BOO patients (**Figure 6A**). Furthermore, the vascular endothelial growth factor (VEGFA) (**Figure 6B**) and lactate dehydrogenase A (LDH-A) (**Figure 6C**), which are regulated by HIF, undergo the initial up-regulation at 2 weeks pBOO followed by a time-dependent decrease. In human patients, the levels of VEGFA and LDHA remain consistently higher than in controls (**Figure 6B**, **6C**).

Discussion

In this study, we describe a revealing comparison between experimentally-induced pBOO in mice and BOO-induced LUTDs in patients, identifying selected changes in miRNAs and mRNAs that are conserved between the two systems. Similar to prior reports we observed that the bladder-to-body weight ratio increased in a time-dependent manner after surgically-induced pBOO compared with sham-operated mice [3, 29]. miRNA expression in the 1st study showed changes after 2 weeks of pBOO but the expression returned to control (sham) levels after 6 weeks of obstruction. Therefore, we performed a longer 2nd study up to 8 weeks pBOO, in order to assess the influence of the time post-obstruction on the gene expression regulation.

We analyzed expression levels of several miRNAs described to be important for hypertrophy and fibrosis. MiR-142-3p and miR-142-5p influence inflammation and immune response, and have also been shown to decrease in mouse models of cardiac hypertrophy. MiR-142-5p targets the acetyltransferase p300, implicated in cardiac growth, and an increase of miR-142 during cardiac growth is critical for cell survival [34, 35]. In our data set, miR-142-5p displayed a biphasic response, increasing at 2 and 6-8 weeks of pBOO but showing the levels close to controls at 4 weeks pBOO. Based on the literature, a reduction in miR-142 is anticipated to cause an increase in cytokine-mediated survival signals and a reduction in apoptosis [35]. MiR-30c was down-regulated at the beginning of obstruction in both studies we report here. Like many other dysregulated miRNAs, miR-30c levels gradually returned to control as obstruction time elapsed, similar to the earlier observations in pBOO rats [22]. In cardiomyocytes miR-30c was shown to inhibit connective tissue growth factor (CTGF) [36], in line with our

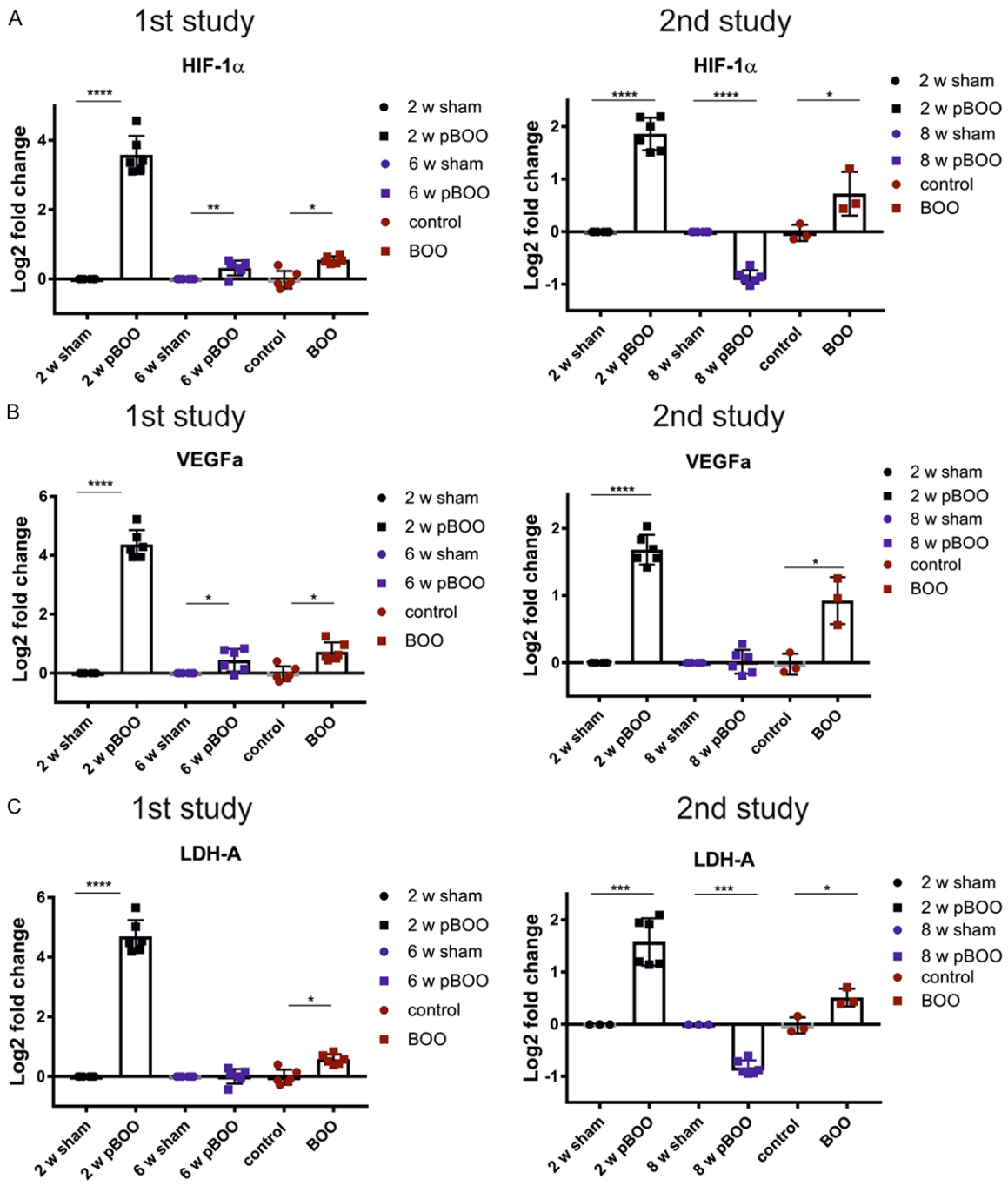

Figure 6. The effect of pBOO on hypoxia-induced gene expression. Gene expression of three hypoxia-induced genes was assessed by qRT-PCR in the 1st and 2nd study mouse bladders and compared with BOO patients' biopsy samples. 2 w sham vs. pBOO (n=4 each), 6 w sham vs. pBOO (n=4 each), BOO (n=18) vs. control (n=6), all samples were measured in triplicates. (A) Levels of HIF1A (B) levels of VEGFA (C) levels of LDH-A. Data are represented as mean ± SD, *P≤0.05, **P≤0.01, ***P≤0.001, ****P≤0.0001.

qRT-PCR data, which show an increase of CTGF in pBOO animals.

In most cases miRNAs, which were selected based on their relevance in human bladder remodeling, were in agreement between mouse pBOO and human BOO patients' samples. We observed that smooth muscle-associated miRNAs, such as miR-1 and miR-133a-3p, miR143/145, which are confirmed to play a role in car-

diac hypertrophy [37, 38] were down-regulated. Overexpression of miR-1 and miR-133 inhibits the development of cardiac hypertrophy [38]. Earlier studies have shown that miR-29b and -29c are significantly reduced in experimental obstruction in animal models [13], in line with this report. Our study did not show conclusive evidence of miR-29b down-regulation in pBOO mice, though we previously demonstrated its reduction in humans with BOO [14]. On the other hand, the pro-fibrotic miRNAs miR-142-3p and miR-21 were up-regulated in both studies performed here, in agreement with the published data on miR-21 increase during renal fibrosis [39]. Interestingly, miR-155-5p was differently expressed between 1st and 2nd study. In the 1st study, after 6 weeks of obstruction miR-155 was enhanced similarly to BOO human patients but in the 2nd study after 8 weeks obstruction it was highly down-regulated. The pro-inflammatory miR-155 is up-regulated during heart failure in patients and loss of miR-155 in fibroblasts showed a protection of ventricular function [40].

Given the inconsistent and sometimes conflicting expression results for individual miRNAs, we compared the expression of important hubs of cell signaling between pBOO mouse bladders and BOO patients' biopsy samples. We found evidence to support similar regulation of mRNAs encoding for pro-fibrotic regulatory proteins in the two systems. For example, CTGF was increased between 4 and 6 weeks of obstruction in mice and in patients with BOO. In line with an adaptive upregulation in response to bladder distension and mechanical stimulation, CTGF is known to be upregulated in cardiomyocytes under conditions of heart failure in rodent models, where it promotes hypertrophy [41]. MYC and MYH-11 were regulated in a biphasic manner in mice and humans. However, contrary to the human data in which these genes were highly upregulated with BOO, we found no evidence of up-regulation of the TNF-α-induced genes PIK3R5, PTGS2, UPK2, and TNFAIP3 following pBOO in mice. Interestingly genes identified as responsive to obstruction, showed differential time- and dose-dependent regulation in the context of cyclophosphamide-induced bladder inflammation. Among these, MYC and VEGFA were upregulated at 96 h following treatment of mice with high-dose Cyp. Consistent with these observations, MYC has been implicated as a driver of metabolic changes in tissues exposed to both mechanical and inflammatory stress in vivo [42, 43]. The discrepancy between human BOO, mouse pBOO and mouse bladder inflammation likely reflects different kinetics of transcriptional regulation. It may also be a reflection of post-operative meloxicam administered to mice following pBOO, which exerts anti-inflammatory activity.

Although hypoxia is a common feature of obstructed bladders in humans [44], our mouse studies showed convincing evidence of hypoxia only at the 2 week time point, with hypoxic gene expression changes reverting to control levels after 6-8 weeks of pBOO. Hypoxia inducible factor (HIF)-1 plays a major role in mediating the response to low oxygen concentration in tissues. The synthesis of HIF-1α is enhanced after pBOO in mice or rats following 6-14 days of obstruction [6, 45]. HIF-1 promotes the transcription of VEGF and angiogenesis, through VEGF-mediated attraction of mature endothelial cells to the hypoxic environment [33]. VEGF is significantly up-regulated in patients with BOO [46] and also in rats within 14 days of obstruction [6]. Overall, the evidence in support of increased hypoxia-induced gene expression during the first 2 weeks of obstruction in different animal models is comparable with the results presented here. Nevertheless, our study in mice with pBOO is, to our knowledge, the first to show that hypoxia-induced changes in gene expression disappear and the levels of up-regulated genes return to normal in a time-dependent manner at later time points (6-8 wk) after obstruction. Notably, there is a strong connection between inflammation and hypoxia, which may explain the up-regulation of hypoxia-induced genes in the first 2 weeks after pBOO surgery [47]. Our miRNA and mRNA expression data suggest an inflammatory trend at the beginning of the obstruction, which subsides at later time points after surgery. Generally, our studies demonstrate that the gene expression dysregulation (both miRNAs and mRNAs) is the strongest at 2 weeks post-obstruction, and the changes gradually return to the control levels. This is in agreement with an earlier observation in pBOO rats, where with the exception of miR-1 and miR-133a, the level of most other tested miRNAs normalized by 6 weeks after pBOO [22].

Based on our results, pBOO leads to an acute hypoxia, and possibly inflammation at the beginning but fails to induce the long-term effects observed in patients with BOO-induced LUTD. Limitations of the study include the different ages of mice versus humans, with changes in human patients likely a reflection of chronic damage to the urinary tract, as well as age-related comorbidities. It will be important in future studies to relate miRNA/mRNA changes to the switch from compensated to decompensated contractility in mouse bladders following pBOO, since miRNAs/mRNAs that are differentially expressed during this transition may represent drivers of pathologic remodeling and fibrosis. Most of miRNAs and mRNAs shown to be regulated in the mouse pBOO studies are known to play a role in development of cardiovascular diseases and may play a similar role in bladder hypertrophy [25]. Nevertheless, the lack of evidence of TNF-α-induced miRNA and mRNA regulation might indicate a different pathophysiological mechanism of organ remodeling in pBOO model compared to the human disease.

Acknowledgements

The authors acknowledge the financial support of the Swiss National Science Foundation (SNSF Grant 320030_156161/1 to KM), the Velux Foundation (Grant 895 to KM) and the National Institutes of Health (R01 DK077195 to RMA). The authors also acknowledge technical support from Stefan Lukianov.

Disclosure of conflict of interest

None.

Address correspondence to: Rosalyn M Adam, Department of Urology, Boston Children's Hospital, Boston, MA, USA. E-mail: rosalyn.adam@childrens.harvard.edu; Katia Monastyrskaya, Urology Research Laboratory, Department of Clinical Research, University of Bern, Switzerland. E-mail: katia.monastyrskaia@dbmr.unibe.ch

References

[1] Kitta T, Kanno Y, Chiba H, Higuchi M, Ouchi M, Togo M, Moriya K and Shinohara N. Benefits and limitations of animal models in partial bladder outlet obstruction for translational research. Int J Urol 2018; 25: 36-44.

[2] Lemack GE, Burkhard F, Zimmern PE, McConnell JD and Lin VK. Physiologic sequelae of partial infravesical obstruction in the mouse: role of inducible nitric oxide synthase. J Urol 1999; 161: 1015-1022.

[3] Austin JC, Chacko SK, DiSanto M, Canning DA and Zderic SA. A male murine model of partial bladder outlet obstruction reveals changes in detrusor morphology, contractility and Myosin isoform expression. J Urol 2004; 172: 1524-1528.

[4] Zderic SA and Chacko S. Alterations in the contractile phenotype of the bladder: lessons for understanding physiological and pathological remodelling of smooth muscle. J Cell Mol Med 2012; 16: 203-217.

[5] Ghafar MA, Shabsigh A, Chichester P, Anastasiadis AG, Borow A, Levin RM and Buttyan R. Effects of chronic partial outlet obstruction on blood flow and oxygenation of the rat bladder. J Urol 2002; 167: 1508-1512.

[6] Ghafar MA, Anastasiadis AG, Olsson LE, Chichester P, Kaplan SA, Buttyan R and Levin RM. Hypoxia and an angiogenic response in the partially obstructed rat bladder. Lab Invest 2002; 82: 903-909.

[7] Iguchi N, Malykhina AP and Wilcox DT. Inhibition of HIF reduces bladder hypertrophy and improves bladder function in murine model of partial bladder outlet obstruction. J Urol 2016; 195: 1250-1256.

[8] Ardekani AM and Naeini MM. The role of MicroRNAs in human diseases. Avicenna J Med Biotechnol 2010; 2: 161-179.

[9] Gheinani AH, Burkhard FC and Monastyrskaya K. Deciphering microRNA code in pain and inflammation: lessons from bladder pain syndrome. Cell Mol Life Sci 2013; 70: 3773-3789.

[10] Sanchez Freire V, Burkhard FC, Kessler TM, Kuhn A, Draeger A and Monastyrskaya K. MicroRNAs may mediate the down-regulation of neurokinin-1 receptor in chronic bladder pain syndrome. Am J Pathol 2010; 176: 288-303.

[11] Monastyrskaya K, Sanchez-Freire V, Hashemi Gheinani A, Klumpp DJ, Babiychuk EB, Draeger A and Burkhard FC. miR-199a-5p regulates urothelial permeability and may play a role in bladder pain syndrome. Am J Pathol 2013; 182: 431-448.

[12] Zhang S, Lv JW, Yang P, Yu Q, Pang J, Wang Z, Guo H, Liu S, Hu J, Li J, Leng J, Huang Y, Ye Z and Wang CY. Loss of dicer exacerbates cyclophosphamide-induced bladder overactivity by enhancing purinergic signaling. Am J Pathol 2012; 181: 937-946.

[13] Ekman M, Bhattachariya A, Dahan D, Uvelius B, Albinsson S and Sward K. Mir-29 repression in bladder outlet obstruction contributes to matrix remodeling and altered stiffness. PLoS One 2013; 8: e82308.

[14] Gheinani AH, Kiss B, Moltzahn F, Keller I, Bruggmann R, Rehrauer H, Fournier CA, Burkhard

FC and Monastyrskaya K. Characterization of miRNA-regulated networks, hubs of signaling, and biomarkers in obstruction-induced bladder dysfunction. JCI Insight 2017; 2: e89560.
[15] Sadegh MK, Ekman M, Krawczyk K, Svensson D, Goransson O, Dahan D, Nilsson BO, Albinsson S, Uvelius B and Sward K. Detrusor induction of miR-132/212 following bladder outlet obstruction: association with MeCP2 repression and cell viability. PLoS One 2015; 10: e0116784.
[16] Duan LJ, Qi J, Kong XJ, Huang T, Qian XQ, Xu D, Liang JH and Kang J. MiR-133 modulates TGF-beta1-induced bladder smooth muscle cell hypertrophic and fibrotic response: implication for a role of microRNA in bladder wall remodeling caused by bladder outlet obstruction. Cell Signal 2015; 27: 215-227.
[17] Hashemi Gheinani A, Burkhard FC, Rehrauer H, Aquino Fournier C and Monastyrskaya K. MicroRNA MiR-199a-5p regulates smooth muscle cell proliferation and morphology by targeting WNT2 signaling pathway. J Biol Chem 2015; 290: 7067-7086.
[18] Kriegel AJ, Liu Y, Fang Y, Ding X and Liang M. The miR-29 family: genomics, cell biology, and relevance to renal and cardiovascular injury. Physiol Genomics 2012; 44: 237-244.
[19] Mott JL, Kurita S, Cazanave SC, Bronk SF, Werneburg NW and Fernandez-Zapico ME. Transcriptional suppression of mir-29b-1/mir-29a promoter by c-Myc, hedgehog, and NF-kappaB. J Cell Biochem 2010; 110: 1155-1164.
[20] Zhou L, Wang L, Lu L, Jiang P, Sun H and Wang H. Inhibition of miR-29 by TGF-beta-Smad3 signaling through dual mechanisms promotes transdifferentiation of mouse myoblasts into myofibroblasts. PLoS One 2012; 7: e33766.
[21] Koeck I, Hashemi Gheinani A, Baumgartner U, Vassella E, Bruggmann R, Burkhard FC and Monastyrskaya K. Tumor necrosis Factor-alpha initiates miRNA-mRNA signaling cascades in obstruction-induced bladder dysfunction. Am J Pathol 2018; 188: 1847-1864.
[22] Ekman M, Albinsson S, Uvelius B and Sward K. MicroRNAs in bladder outlet obstruction: Relationship to growth and matrix remodelling. Basic Clin Pharmacol Toxicol 2016; 119 Suppl 3: 5-17.
[23] Metcalfe PD, Wang J, Jiao H, Huang Y, Hori K, Moore RB and Tredget EE. Bladder outlet obstruction: progression from inflammation to fibrosis. BJU Int 2010; 106: 1686-1694.
[24] Altuntas CZ, Daneshgari F, Izgi K, Bicer F, Ozer A, Sakalar C, Grimberg KO, Sayin I and Tuohy VK. Connective tissue and its growth factor CTGF distinguish the morphometric and molecular remodeling of the bladder in a model of neurogenic bladder. Am J Physiol Renal Physiol 2012; 303: F1363-1369.
[25] Koeck I, Burkhard FC and Monastyrskaya K. Activation of common signaling pathways during remodeling of the heart and the bladder. Biochem Pharmacol 2016; 102: 7-19.
[26] Sadegh MK, Ekman M, Rippe C, Uvelius B, Sward K and Albinsson S. Deletion of Dicer in smooth muscle affects voiding pattern and reduces detrusor contractility and neuroeffector transmission. PLoS One 2012; 7: e35882.
[27] Xin M, Small EM, Sutherland LB, Qi X, McAnally J, Plato CF, Richardson JA, Bassel-Duby R and Olson EN. MicroRNAs miR-143 and miR-145 modulate cytoskeletal dynamics and responsiveness of smooth muscle cells to injury. Genes Dev 2009; 23: 2166-2178.
[28] Malmgren A, Sjogren C, Uvelius B, Mattiasson A, Andersson KE and Andersson PO. Cystometrical evaluation of bladder instability in rats with infravesical outflow obstruction. J Urol 1987; 137: 1291-1294.
[29] Vasquez E, Cristofaro V, Lukianov S, Burkhard FC, Gheinani AH, Monastyrskaya K, Bielenberg DR, Sullivan MP and Adam RM. Deletion of neuropilin 2 enhances detrusor contractility following bladder outlet obstruction. JCI Insight 2017; 2: e90617.
[30] Baumgartner U, Berger F, Hashemi Gheinani A, Burgener SS, Monastyrskaya K and Vassella E. miR-19b enhances proliferation and apoptosis resistance via the EGFR signaling pathway by targeting PP2A and BIM in non-small cell lung cancer. Mol Cancer 2018; 17: 44.
[31] Lassmann J, Sliwoski J, Chang A, Canning DA and Zderic SA. Deletion of one SERCA2 allele confers protection against bladder wall hypertrophy in a murine model of partial bladder outlet obstruction. Am J Physiol Regul Integr Comp Physiol 2008; 294: R58-65.
[32] Leventhal L and Strassle B. A model of cystitis pain in the mouse. Curr Protoc Pharmacol 2008; Chapter 5: Unit 5 52.
[33] Iguchi N, Hou A, Koul HK and Wilcox DT. Partial bladder outlet obstruction in mice may cause E-cadherin repression through hypoxia induced pathway. J Urol 2014; 192: 964-972.
[34] Sharma S, Liu J, Wei J, Yuan H, Zhang T and Bishopric NH. Repression of miR-142 by p300 and MAPK is required for survival signalling via gp130 during adaptive hypertrophy. EMBO Mol Med 2012; 4: 617-632.
[35] Shrestha A, Mukhametshina RT, Taghizadeh S, Vasquez-Pacheco E, Cabrera-Fuentes H, Rizvanov A, Mari B, Carraro G and Bellusci S. MicroRNA-142 is a multifaceted regulator in organogenesis, homeostasis, and disease. Dev Dyn 2017; 246: 285-290.
[36] Duisters RF, Tijsen AJ, Schroen B, Leenders JJ, Lentink V, van der Made I, Herias V, van Leeuwen RE, Schellings MW, Barenbrug P, Maessen JG, Heymans S, Pinto YM and Creemers EE.

miR-133 and miR-30 regulate connective tissue growth factor: implications for a role of microRNAs in myocardial matrix remodeling. Circ Res 2009; 104: 170-178, 176p following 178.
[37] Cordes KR, Srivastava D and Ivey KN. MicroRNAs in cardiac development. Pediatr Cardiol 2010; 31: 349-356.
[38] Care A, Catalucci D, Felicetti F, Bonci D, Addario A, Gallo P, Bang ML, Segnalini P, Gu Y, Dalton ND, Elia L, Latronico MV, Hoydal M, Autore C, Russo MA, Dorn GW 2nd, Ellingsen O, Ruiz-Lozano P, Peterson KL, Croce CM, Peschle C and Condorelli G. MicroRNA-133 controls cardiac hypertrophy. Nat Med 2007; 13: 613-618.
[39] Meng XM, Chung AC and Lan HY. Role of the TGF-beta/BMP-7/Smad pathways in renal diseases. Clin Sci (Lond) 2013; 124: 243-254.
[40] Cao RY, Li Q, Miao Y, Zhang Y, Yuan W, Fan L, Liu G, Mi Q and Yang J. The emerging role of MicroRNA-155 in cardiovascular diseases. Biomed Res Int 2016; 2016: 9869208.
[41] Panek AN, Posch MG, Alenina N, Ghadge SK, Erdmann B, Popova E, Perrot A, Geier C, Dietz R, Morano I, Bader M and Ozcelik C. Connective tissue growth factor overexpression in cardiomyocytes promotes cardiac hypertrophy and protection against pressure overload. PLoS One 2009; 4: e6743.
[42] Ahuja P, Zhao P, Angelis E, Ruan H, Korge P, Olson A, Wang Y, Jin ES, Jeffrey FM, Portman M and Maclellan WR. Myc controls transcriptional regulation of cardiac metabolism and mitochondrial biogenesis in response to pathological stress in mice. J Clin Invest 2010; 120: 1494-1505.
[43] Wang R, Dillon CP, Shi LZ, Milasta S, Carter R, Finkelstein D, McCormick LL, Fitzgerald P, Chi H, Munger J and Green DR. The transcription factor Myc controls metabolic reprogramming upon T lymphocyte activation. Immunity 2011; 35: 871-882.
[44] Koritsiadis G, Tyritzis SI, Koutalellis G, Lazaris AC and Stravodimos K. The effect of alpha-blocker treatment on bladder hypoxia inducible factor-1 alpha regulation during lower urinary tract obstruction. Int Braz J Urol 2010; 36: 86-94.
[45] Ekman M, Uvelius B, Albinsson S and Sward K. HIF-mediated metabolic switching in bladder outlet obstruction mitigates the relaxing effect of mitochondrial inhibition. Lab Invest 2014; 94: 557-568.
[46] Barbosa J, Reis ST, Nunes M, Ferreira YA, Leite KR, Nahas WC, Srougi M and Antunes AA. The obstructed bladder: expression of collagen, matrix metalloproteinases, muscarinic receptors, and angiogenic and neurotrophic factors in patients with benign prostatic hyperplasia. Urology 2017; 106: 167-172.
[47] Ramakrishnan S, Anand V and Roy S. Vascular endothelial growth factor signaling in hypoxia and inflammation. J Neuroimmune Pharmacol 2014; 9: 142-160.